MOLECULAR TOXICOLOGY

Autophagy (but not metabolism) is a key event in mitoxantrone-induced cytotoxicity in differentiated AC16 cardiac cells

Ana Reis-Mendes[1,2] · Félix Carvalho[1,2] · Fernando Remião[1,2] · Emília Sousa[3,4] · Maria de Lourdes Bastos[1,2] · Vera Marisa Costa[1,2]

Abstract

Mitoxantrone (MTX) is an antineoplastic agent used to treat advanced breast cancer, prostate cancer, acute leukemia, lymphoma and multiple sclerosis. Although it is known to cause cumulative dose-related cardiotoxicity, the underlying mechanisms are still poorly understood. This study aims to compare the cardiotoxicity of MTX and its' pharmacologically active metabolite naphthoquinoxaline (NAPHT) in an in vitro cardiac model, human-differentiated AC16 cells, and determine the role of metabolism in the cardiotoxic effects. Concentration-dependent cytotoxicity was observed after MTX exposure, affecting mitochondrial function and lysosome uptake. On the other hand, the metabolite NAPHT only caused concentration-dependent cytotoxicity in the MTT reduction assay. When assessing the effect of different inhibitors/inducers of metabolism, it was observed that metyrapone (a cytochrome P450 inhibitor) and phenobarbital (a cytochrome P450 inducer) slightly increased MTX cytotoxicity, while 1-aminobenzotriazole (a suicide cytochrome P450 inhibitor) decreased fairly the MTX-triggered cytotoxicity in differentiated AC16 cells. When focusing in autophagy, the mTOR inhibitor rapamycin and the autophagy inhibitor 3-methyladenine exacerbated the cytotoxicity caused by MTX and NAPHT, while the autophagy blocker, chloroquine, partially reduced the cytotoxicity of MTX. In addition, we observed a decrease in p62, beclin-1, and ATG5 levels and an increase in LC3-II levels in MTX-incubated cells. In conclusion, in our in vitro model, neither metabolism nor exogenously given NAPHT are major contributors to MTX toxicity as seen by the residual influence of metabolism modulators used on the observed cytotoxicity and by NAPHT's low cytotoxicity profile. Conversely, autophagy is involved in MTX-induced cytotoxicity and MTX seems to act as an autophagy inducer, possibly through p62/LC3-II involvement.

Keywords Mitoxantrone · Metabolism · Naphthoquinoxaline metabolite · Differentiated AC16 cardiac cells · Autophagy · Cardiotoxicity

Abbreviations

1-ABT	1-Aminobenzotriazole
3- MA	3-Methyladenine
ATG5	Autophagy related 5
CQ	Chloroquine
DAS	Diallyl sulfide

✉ Vera Marisa Costa
  veramcosta@ff.up.pt

  Ana Reis-Mendes
  afreis.mendes@gmail.com

  Félix Carvalho
  felixdc@ff.up.pt

  Fernando Remião
  remiao@ff.up.pt

  Emília Sousa
  esousa@ff.up.pt

  Maria de Lourdes Bastos
  mlbastos@ff.up.pt

[1] Associate Laboratory i4HB, Institute for Health and Bioeconomy, Faculty of Pharmacy, University of Porto, 4050-313 Porto, Portugal

[2] Department of Biological Sciences, UCIBIO - Applied Molecular Biosciences Unit, REQUIMTE, Laboratory of Toxicology, Faculty of Pharmacy, University of Porto, Rua de Jorge Viterbo Ferreira, 228, 4050-313 Porto, Portugal

[3] Laboratory of Organic and Pharmaceutical Chemistry, Chemistry Department, Faculty of Pharmacy, University of Porto, 4050-313 Porto, Portugal

[4] CIIMAR—Interdisciplinary Centre of Marine and Environmental Research, 4450-208 Porto, Portugal

DMEM/F-12	Dulbecco´s modified Eagle´s medium/ nutrient F-12 Ham
DMSO	Dimethyl sulfoxide
GAPDH	Glyceraldehyde-3-phosphate dehydrogenase
LC3	Microtubule-associated protein 1A/1B-light chain 3
MTT	4,5-Dimethylthiazol-2-yl)-2,5-diphenyl tetrazolium bromide
MTP	Metyrapone
MTX	Mitoxantrone
NAPHT	Naphthoquinoxaline
NR	Neutral red
OD	Optic density
PHB	Phenobarbital
PI3K-III	Class III phosphatidylinositol 3-kinase
RAP	Rapamycin
RIF	Rifampicin (RIF)
SD	Standard deviation

Introduction

Mitoxantrone (MTX) is an antineoplastic agent from the synthetic anthracenediones family (Reis-Mendes et al. 2015). MTX interferes with DNA synthesis and repair by intercalating through hydrogen bonding, leading to crosslinks and strand breaks (Reis-Mendes et al. 2015). Moreover, MTX has powerful immunosuppressive and immunomodulatory properties, as it abrogates T helper activity, increases T suppressor cell function, inhibits B lymphocyte function, and macrophage proliferation (Fox 2004; Scott and Figgitt 2004). MTX is used to treat several types of cancers and aggressive or refractory multiple sclerosis. Nevertheless, its use is accompanied by a high incidence of cardiotoxicity, dependent on MTX lifelong cumulative dose (Reis-Mendes et al. 2015). Such cardiotoxicity is often characterized by arrhythmias, electrocardiographic changes, and heart failure (Reis-Mendes et al. 2015).

Regarding MTX pharmacokinetic properties, it is metabolized primarily in the liver. In the first 5 days, only 20–32% of administered MTX is excreted in urine (6–11%) and feces (13–25%). Regarding the urinary excretion in cancer patients, 65% is excreted as unchanged MTX and the remaining 35% are excreted in the form of metabolites (Alberts et al. 1985; Reis-Mendes et al. 2015). Moreover, MTX accumulates extensively in highly perfused organs, including the heart (An and Morris 2010). Even if the majority of MTX metabolism is hepatic, the metabolites formed can reach the heart due to their distribution through the blood. Moreover, the heart is an organ that expresses cytochrome P450 (CYP450) enzymes and NADPH cytochrome reductase (Duthie and Grant 1989) among other enzymatic

complexes, which can generate metabolites *in loco* that may cause cardiac toxicity (Wormhoudt et al. 1999). Regarding MTX metabolism, the two-electron reduction is considered the preferential pathway. MTX main metabolic products are the naphthoquinoxaline (NAPHT) metabolite and its oxidation products, the MTX mono- and dicarboxylic derivatives. The MTX conjugates with glutathione and glucuronic acid have also been described (Reis-Mendes et al. 2015; Rossato et al. 2013a). Regarding the interspecies variability, mono- and dicarboxylic acid derivatives of MTX are major human urinary products, while in rats they are residual (Blanz et al. 1991a, b; Ehninger et al. 1990). However, these have no pharmacological anticancer activity (Chiccarelli et al. 1986). Nonetheless, when CYP450-mediated metabolism is inhibited, MTX toxicity is prevented in different cell models (Duthie and Grant 1989; Li et al. 1995; Mewes et al. 1993), advocating for a role of metabolism in its pharmacological activity. The metabolite NAPHT is known to be a product of the biotransformation of MTX in vivo through systems containing CYP450, DT-diaphorase, NADPH cytochrome reductases, and peroxidases (Brück and Brück 2011). This metabolite was already identified in human, rat, and pig urine after MTX intravenous administration (Blanz et al. 1991b) and has been reported to have a significant role in the pharmacological anticancer activity of MTX (Feofanov et al. 1997b; Mewes et al. 1993; Panousis et al. 1994, 1997).

In summary, the heart does not just receive metabolites from the liver, but has its own metabolic capacity, although its importance for the MTX-inflicted cardiotoxicity is not yet known. Overall, the underlying mechanisms of MTX cardiotoxicity are poorly understood and the potential toxicity of the MTX metabolite NAPHT is scarcely investigated. We have done a previous work showing that NAPHT has lower toxicity when compared with MTX in H9c2 differentiated cells (Reis-Mendes et al. 2017), but in undifferentiated H9c2 cells, MTX metabolism is partially responsible for its cytotoxicity (Rossato et al. 2013a).

Autophagy is a regulated catabolic mechanism that involves the delivery of cytoplasmic cargo sequestered inside double-membrane vesicles to the lysosome and is highly controlled by some autophagy-related genes (Parzych and Klionsky 2014), playing dual and intrinsic roles in cell death or survival. Autophagy has been characterized as an essential cellular process in the heart, removing protein aggregates and damaged organelles, protecting against famine, excessive β-adrenergic stimulation, and ischemia (De Meyer and Martinet 2009). Since the heart has cardiomyocytes that are terminally differentiated non-dividing cells, the correct function of the autophagic degradation process is essential for the maintenance of myocyte homeostasis (Cuervo 2004). Though autophagy is generally viewed as a survival mechanism, excessive autophagy has been associated with cardiac disease, including ischemia/reperfusion, cardiac oxidative

stress, and heart failure (Hariharan et al. 2011; Takemura et al. 2006; Valentim et al. 2006). In human failing hearts, both apoptosis and massive autophagy were detected (Kostin et al. 2003). The autophagic cell death process in cardiomyocytes takes place through either uncontrolled degradation of cargo materials due to increased autophagic flux or excessive build-up of autophagosomes caused by an imbalance between autophagy initiation and lysosomal degradation (Ikeda et al. 2022). Although MTX has been reported to deregulate autophagy in in vitro models of cancer (Guan et al. 2020; Xie et al. 2020), the role of autophagy on MTX-induced cardiotoxicity (or of its pharmacologically active metabolite, NAPHT, for that matter) has not been described as far as we know. Therefore, this study aimed to: first, compare the toxicity of MTX and its pharmacologically active and commercially available metabolite NAPHT in an in vitro cardiac model, differentiated human AC16 cells, and, second, to determine whether autophagy has any role in the observed effects.

Materials and methods

AC16 human cardiomyocytes cell line was obtained from Sigma-Aldrich (St. Louis, MO, USA). All plastic sterile materials used in cell culture were obtained from Corning Star (Corning, NY, USA). NAPHT was obtained from MeD CHEM101 (Plymouth Meeting, Pennsylvania). MTX dihydrochloride, neutral red (NR) solution, sodium bicarbonate, gelatine from bovine skin, trypan blue solution 0.4% (w/v), trypsin/ethylenediaminetetraacetic acid solution, acridine orange, ethidium bromide, bovine serum albumin, dimethyl sulfoxide (DMSO), Hoechst 33258 solution, 3-methyladenine (3-MA), chloroquine (CQ), rapamycin (RAP), diallyl sulfide (DAS), metyrapone (MTP), 1-aminobenzotriazole (1-ABT), rifampicin (RIF), phenobarbital (PHB) were obtained from Sigma-Aldrich (Germany). Paraformaldehyde 4% and 3-(4,5-dimethylthiazol-2-yl)-2,5-diphenyl tetrazolium bromide (MTT) were obtained from Alfa Aesar, and fibronectin from bovine plasma was obtained from Thermo Fisher Scientific (Kandel, Germany). Phosphate-buffered saline, penicillin/streptomycin, and Hank's balanced salt solution were obtained from Biochrom (Berlin, Germany). Dulbecco´s Modified Eagle´s Medium/Nutrient F-12 Ham (DMEM/F-12) powder, horse serum heat-inactivated, and fetal bovine serum (FBS) heat-inactivated were obtained from Alfagene (Carcavelos, Portugal). Enhanced chemiluminescence (ECL) reagents, and 0.45 µm Amersham Protran nitrocellulose blotting membrane were obtained from GE Healthcare Bio-Sciences (Pittsburgh, PA, USA). Protein assay kit Bio-Rad RC DC was obtained from Bio-Rad Laboratories (USA).

Cell culture experimental protocols

The toxicological evaluation of MTX and NAPHT was performed in vitro, using the human cardiomyocyte cell line AC16. AC16 cells were maintained in DMEM/F-12 medium (supplemented with 12.5% FBS, 1% penicillin and 100 µg/mL streptomycin), at 37 °C in a 5% CO_2 humidified atmosphere. Cell passaging was done by trypsinization, and the cells were used until the tenth passage, as recommended (Davidson et al. 2005). When the cell population reached 80–90% confluence, experiments were performed. AC16 cells were seeded at a density of 32.5×10^4 cells/cm^2 in coated surfaces with 12.5 µg/mL fibronectin in 0.02% gelatine, for at least 1 h at 37 °C (Dionísio et al. 2022). The differentiation procedure began 24 h after seeding when AC16 cells were exposed to a differentiated medium (DMEM/F12 medium supplemented with 2% horse serum and 1% antibiotics) for 24 h (Davidson et al. 2005). Drug exposure in differentiated cells never surpassed 48 h.

MTX was prepared each month in sterile phosphate-buffered saline without Ca^{2+} and Mg^{2+} and stored at -20 °C. NAPHT was dissolved in DMSO and stored at -20 °C. MTX and NAPHT solutions were not given more than three cycles of freezing/thawing. Moreover, in all NAPHT experiments, an assay with DMSO was run in parallel with the maximum concentration *per* well of 0.1% *v/v*.

Cytotoxicity tests

For determination of the cytotoxic effect of MTX and NAPHT (or the influence of inhibitors or inducers) on the differentiated AC16 cells, two assays were performed: the MTT reduction and the NR uptake assays. To perform either MTT or NR cytotoxicity assays, cells were seeded in 48-well plates, differentiated and incubated with MTX (0.5 to 10 µM) or NAPHT (1 to 10 µM) for 24 or 48 h. In another set of assays, differentiated AC16 cells were pre-incubated with CYP450 inhibitors: a competitive CYP450 inhibitor, MTP (0.5 mM) (Sampath-Kumar et al. 1997), a suicide CYP450 inhibitor, 1-ABT (0.5 mM) (Linder et al. 2009), a CYP2E1 inhibitor, DAS (50 µM) (Jin et al. 2013), and inducers: a strong CYP3A4 inducer, RIF (10 µM) (Bulutoglu et al. 2019; Lin 2006), a CYP2B6 inducer and also aldo–keto reductases inhibitor, PHB (1 mM) (Behnia and Boroujerdi 1999; Deng et al. 2013; Lin 2006) for 1 h at 37 °C before MTX was added.

Finally, autophagy was evaluated using the NR uptake assay, since it relates to lysosome function: it is based on the ability of viable cells to incorporate and bind to the supravital dye NR in the lysosomes (Repetto et al. 2008). Therefore, the effects of the autophagy inhibitor, 3-MA (2.5 mM) (Soares et al. 2014) or blocker, CQ (10 µM) (Bik et al. 2021), and of an autophagy activator, RAP (0.1 µM) (Guan et al.

2020) were evaluated. These compounds were added 1 h before cells' exposure to MTX or NAPHT.

MTT reduction assay

The MTT colorimetric assay is based on the reduction of the tetrazolium salt to formazans by dehydrogenases and it was performed as previously described (Dionísio et al. 2022). The percentage of MTT reduction in control cells was set at 100% and the values of each treatment are expressed as a percentage of control cells.

NR uptake assay

The amount of NR dye incorporated into the cells usually represents their lysosomal functionality, as this dye easily enters cell membranes and is retained within lysosomes (Repetto et al. 2008). It was performed as previously described within the group (Dionísio et al. 2022). The percentage of NR uptake of control cells was set at 100% and the values of each treatment are expressed as a percentage of control cells.

Microscopic observation of the cells

Morphology evaluation

For the morphological microscopy evaluation, differentiated AC16 cells were seeded in 24-well plates and incubated with MTX (0.5 to 10 μM) or NAPHT (1 to 10 μM) for 48 h. Next, cells' morphology was evaluated by contrast phase microscopy, using a Nikon Eclipse TS100 equipped with a Nikon DS-Fi1 camera (Tokyo, Japan).

Hoechst nuclear staining

Hoechst staining was used to assess the effect of MTX or NAPHT on nuclear morphology of differentiated AC16 cells, as described (Dionísio et al. 2022). The stained nuclei were examined in a Lionheart FX microscope (Biotek, Winooski, Vermont, USA) using a blue fluorescence filter ($\lambda_{\text{excitation}} = 377$ nm and $\lambda_{\text{emission}} = 447$ nm). Twelve photos were taken *per* condition, from 3 independent experiments.

Acridine orange and ethidium bromide staining

Acridine orange and ethidium bromide staining were also performed. Viable cells show an intact green nucleus, early apoptotic cells exhibit a bright green nucleus with condensed or fragmented chromatin, while late apoptotic cells show a condensed or fragmented orange chromatin. Necrotic cells display a uniformly orange-stained nucleus (McGahon 1995). After a 24-h incubation with MTX or NAPTH, the

staining was made as described (Dionísio et al. 2022), and the cells were observed in a Nikon Eclipse TS100 equipped with a Nikon DS-Fi1 camera, using a standard filter for fluorescein ($\lambda_{\text{excitation}} = 485$ nm and $\lambda_{\text{emission}} = 525$ nm). Twelve photos were taken *per* condition, from 3 independent experiments.

Western blot analysis

For western blotting, differentiated AC16 cells were seeded in 6-well plates and exposed to MTX (1, 5, or 10 μM) and NAPHT (1, 5, or 10 μM) for 48 h. Two wells *per* condition were gathered and cells were lysed in RIPA buffer [50 mM Tris–HCl, 150 mM NaCl, 1% Triton X-100 (*v/v*), 0.5% sodium deoxycholate (*w/v*), and 0.1% SDS (*w/v*)], pH 8.0, [supplemented with 0.25 mM phenylmethanesulfonyl fluoride, 1 mM sodium metavanadate, 10 mM sodium fluoride, 1 mM DL-dithiothreitol and 0.5% (*v/v*) complete protease inhibitor cocktail] through sonication and were kept at −80 °C until analysis. Protein quantification was made by the DC protein quantification assay (BioRad) following the manufacturer's instructions. Equal protein amounts (20 μg) were used and ran in 12.5% or 15% SDS-PAGE gels, which were then transferred onto PVDF membranes by Trans-Blot® Turbo™ Transfer System (Bio-Rad, Hercules, CA, USA) using the protocol Low MW (5 min) and Mixed MW (7 min) with voltage 2.5A constant, up to 25 V. The obtained membranes were blocked with 5% skim milk diluted in TBS-Tween for 1 h. The antibodies [rabbit monoclonal anti-APG5L/Autophagy Related 5 (ATG5) (ab108327, Abcam), rabbit polyclonal anti-microtubule-associated protein 1A/1B-light chain 3 (LC3) (L7433, Sigma), mouse monoclonal anti-p62 (ab56416, Abcam), rabbit monoclonal anti-Beclin 1 (#3495, Cell Signaling Technology) and rabbit polyclonal anti-glyceraldehyde-3-phosphate dehydrogenase (GAPDH) (1:1000, ab9485, Abcam)] were incubated at 4 °C overnight using the 1:1000 dilution. In the next day, the membranes were incubated with secondary antibodies [Goat anti-rabbit IgG-horseradish peroxidase (1:5000, ab97051, Abcam) and mouse anti-mouse IgG-horseradish peroxidase (1:2000, sc516102, Santa Cruz)]. An ECL-Plus detection reagent was used to detect the signal of protein expression using the ChemiDoc Imaging System version 2.3.0.07 (Bio-Rad, Hercules, CA, USA). The obtained images were analyzed with Image Lab software version 6.0.1 (Bio-Rad, Hercules, CA, USA). GAPDH was used as a loading control. Three independent experiments were done.

Statistical analysis

Results are expressed as mean ± standard deviation (SD). When using different concentrations at 2 different timepoints (24 and 48 h), a two-way ANOVA test was performed,
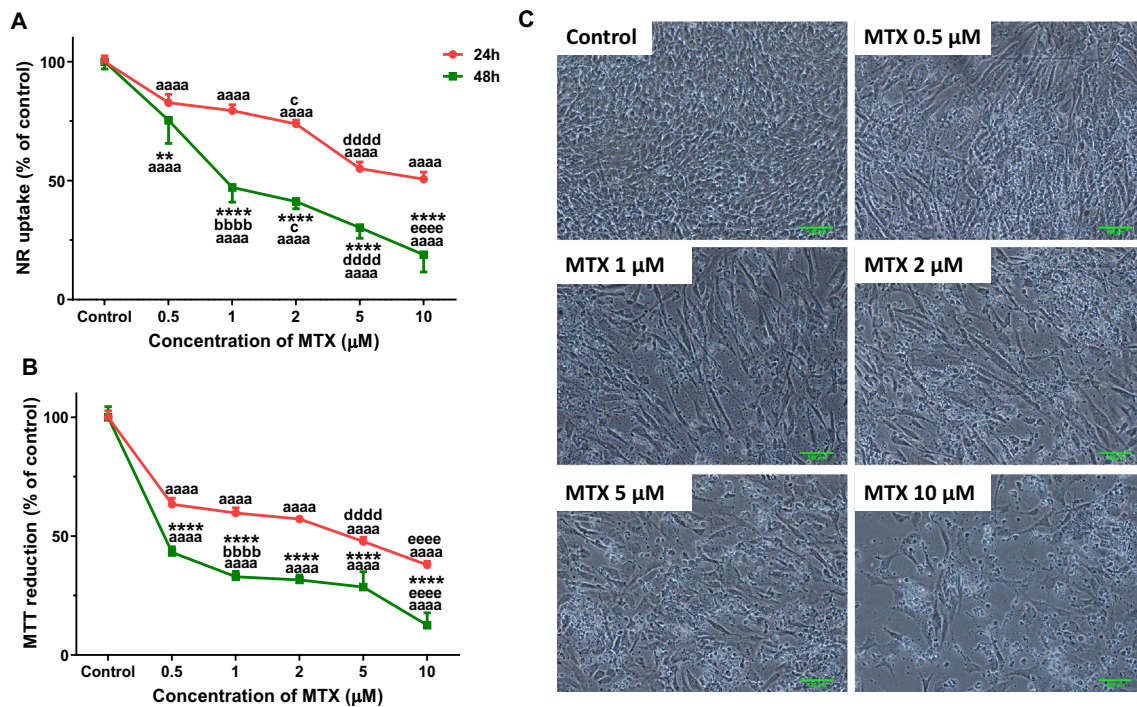
Fig. 1 Lysosomal and mitochondrial dysfunction evaluated by (**A**) the NR uptake and **B** the MTT reduction assays. **A**, **B** Differentiated AC16 cells incubated with 0.5, 1, 2, 5 or 10 μM of MTX for 24 and 48 h. Results are presented as mean ± SD of 3–5 independent experiments (total of 12–20 wells). Statistical analyses were performed using the two-way ANOVA test, followed by the Tukey's post hoc test ($^{aaaa}p < 0.0001$ *versus* control; $^{bbbb}p < 0.0001$ *versus* 0.5 μM; $^{c}p < 0.05$, $^{ccc}p < 0.001$ *versus* 1 μM; $^{dddd}p < 0.0001$ *versus* 2 μM; $^{e}p < 0.05$, $^{ee}p < 0.01$, $^{eeee}p < 0.0001$ *versus* 5 μM; in the same time point) and ($^{**}p < 0.01$, $^{****}p < 0.0001$ *versus* 24 h and $^{####}p < 0.0001$ *versus* 48 h; in the same concentration. **C** Phase-contrast microphotographs of control and MTX-incubated differentiated AC16 cells after 48 h. Images are representative of 3 independent experiments (scale bar represents 100 μm)

followed by the Tukey's post hoc test, when a significant *p* was reached ($p < 0.05$). To assess data normality on assays at one-time point, the D'Agostino & Pearson normality test was performed. If results were normal, a one-way ANOVA test was performed, followed by the Sidak's post hoc test, when a significant *p* was reached ($p < 0.05$). The Kruskal–Wallis test was performed when the data did not follow a normal distribution, followed by Dunn's post hoc test. In the western blot data, statistical comparisons were made using the one-way ANOVA test, followed by the Sidak's post hoc test to compare with control group. Statistical significance was considered when *p* values < 0.05. To perform the statistical analysis, the GraphPad Prism 8.0 software program (San Diego, CA, USA) was used. Details of statistical analysis can be found in the figure's legends.

Results

Mitoxantrone produced a time- and concentration-dependent mitochondrial and lysosome uptake dysfunction in differentiated AC16 cells

Differentiated AC16 cells were exposed to different concentrations (0.5 to 10 μM) of MTX for 24 and 48 h. MTX caused cytotoxicity in a concentration-dependent manner in the assays assessing mitochondrial and lysosome uptake dysfunction. At 24 h, MTX caused small but significant changes of cytotoxicity when compared to control cells, and this effect increased at 48 h, as can be seen in Fig. 1. Regarding the NR uptake assay at 24 h, the values were: 0.5 μM: 82.74 ± 3.53%, 1 μM: 79.42 ± 2.45%, 2 μM: 73.83 ± 1.58%, 5 μM: 55.04 ± 2.79%, and 10 μM: 50.04 ± 2.79%, when compared to control cells (100.00 ± 2.45%) (Fig. 1A). At 48 h, the values of NR uptake were: 0.5 μM: 75.39 ± 9.72%, 1 μM: 47.17 ± 6.24%, 2 μM: 41.21 ± 3.06%, 5 μM: 30.25 ± 4.45%, and 10 μM: 18.89 ± 7.28%, when compared to control cells (100.00 ± 3.11%) (Fig. 1A).
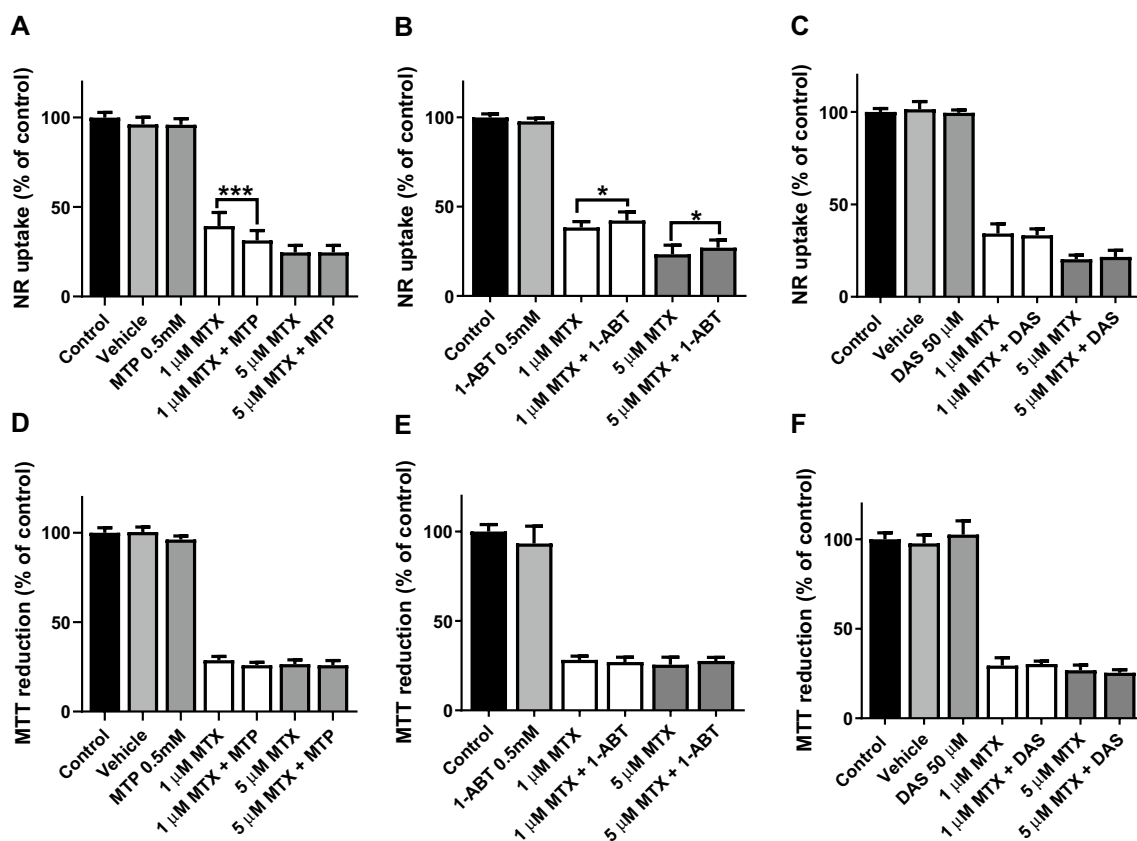
Fig. 2 Lysosomal and mitochondrial dysfunction evaluated by the NR uptake (**A–C**) and the MTT reduction (**D–F**) assays, respectively, in differentiated AC16 cells exposed to 1 or 5 μM of MTX for 48 h with or without (**A, D**) metyrapone (MTP) (0.5 mM final concentration), (**B, E**) 1-aminobenzotriazole (1-ABT) (0.5 mM final concentration), or (**C, F**) diallyl sulfide (DAS) (50 μM final concentration). Results are presented as mean ± SD of 3–4 independ-ent experiments (total of 12–16 wells). The statistical analyses per-formed were: (**C–F**) Kruskal–Wallis test, followed by the Dunn's post hoc test or (**A, B**) one-way ANOVA test, followed by the Sidak's post hoc test (***$p < 0.001$, 1 μM MTX *versus.* 1 μM MTX + MTP) and (*$p < 0.05$, 1 or 5 μM MTX *versus.* 1 or 5 μM MTX + 1-ABT). DMSO (final concentration of 0.1% *v/v*) was used as vehicle

Concerning the MTT reduction assay at 24 h, the val-ues were: 0.5 μM: $63.40 \pm 2.56\%$, 1 μM: $59.71 \pm 2.19\%$, 2 μM: $57.19 \pm 1.50\%$, 5 μM: $47.72 \pm 1.85\%$, and 10 μM: $37.88 \pm 1.54\%$, when compared to control cells ($100.00 \pm 2.73\%$). At 48 h, the values of MTT reduc-tion were: 0.5 μM: $43.14 \pm 2.33\%$, 1 μM: $32.90 \pm 2.25\%$, 2 μM: $31.56 \pm 2.09\%$, 5 μM: $28.59 \pm 6.47\%$, and 10 μM: $12.53 \pm 5.19\%$, when compared to control cells ($100.00 \pm 4.42\%$) (Fig. 1B). The observed cytotoxicity induced by MTX was higher when it was evaluated by the MTT reduction assay than by the NR uptake assay.

Regarding phase-contrast microscopy at 48 h, MTX caused cellular damage, with evident cellular debris, and round and detached cells. The differentiated AC16 cells exposed to 1–10 μM of MTX showed signs of membrane integrity loss and substantial decreases in cell number. There were roughly 50% fewer attached cells after incubation with MTX in some concentrations (1, 2, 5 and 10 μM [Fig. 1C]).

No significant signs of nuclear alteration were found in the Hoechst staining at 48 h when compared to control (Figure S1). In the ethidium bromide/acridine orange staining, the number of cells largely decreased as MTX concentration increased, but cells present in the field maintained a green nucleus, although with evident cytoplasmic injury (Figure S2). The two lowest MTX concentration show some signs of early apoptosis, with condensed nuclei.

Metyrapone increased and 1-aminobenzotriazole decreased the cytotoxicity caused by MTX

Differentiated AC16 cells were pre-incubated with CYP450 inhibitors (MTP, 1-ABT or DAS) for 1 h at 37 °C before MTX was added. In the NR uptake assay, the competitive CYP450 inhibitor MTP (0.5 mM) (Sampath-Kumar et al. 1997) increased the cytotoxicity induced by MTX 1 μM as can be seen in Fig. 2A. In the MTT assay, MTP did not

Fig. 3 Mitochondrial and lysosomal dysfunction evaluated by the (**A, B**) NR uptake and (**C, D**) the MTT reduction assays, respectively, in differentiated AC16 cells incubated with 1 or 5 μM of MTX for 48 h with or without: (**A, C**) phenobarbital (PHB) (1 mM final concentration) or (**B, D**) rifampicin (RIF) (10 μM final concentration). Results are presented as mean ± SD of 3–4 independent experiments (total of 12–15 wells). The statistical analyses performed were: (**A, B**) one-way ANOVA test, followed by the Sidak's post hoc test or (**C, D**) Kruskal–Wallis test, followed by the Dunn's post hoc test (**$p < 0.01$, 1 or 5 μM MTX *versus* 1 or 5 μM MTX + PHB)
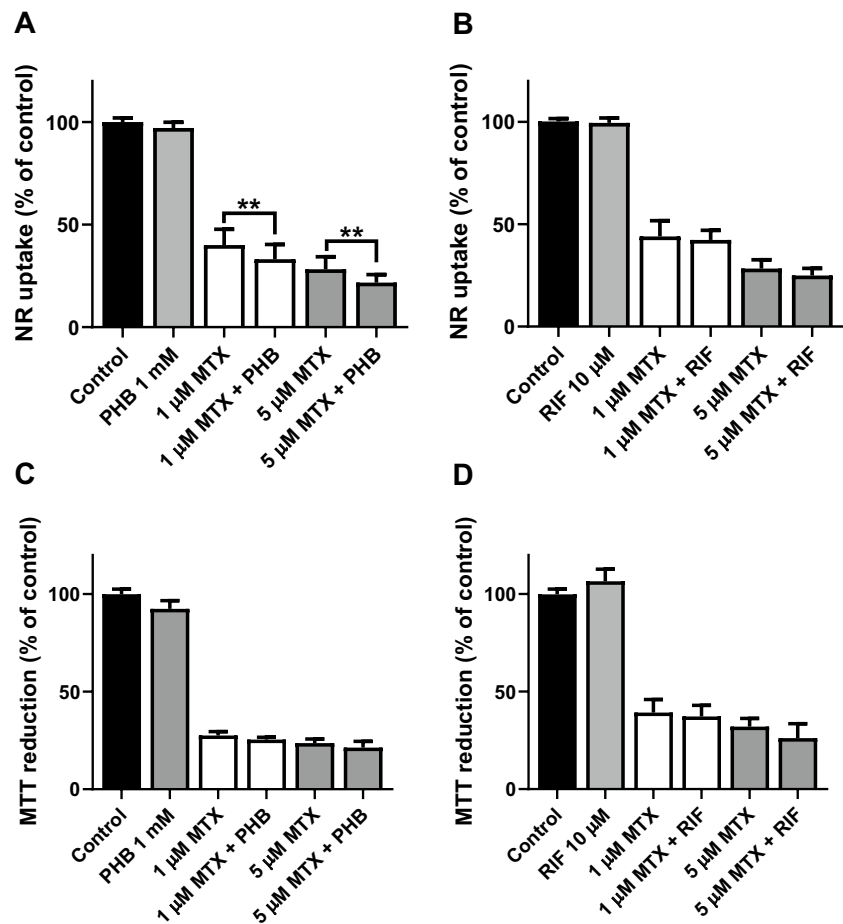
change the MTX-induced cytotoxicity at 48 h (Fig. 2D). The incubation of MTP (0.5 mM) or DMSO (inhibitor vehicle) per se did not cause any toxicity when compared to control conditions in both cytotoxicity tests performed.

At 48 h, 1-ABT, a suicide CYP450 inhibitor (0.5 mM) (Linder et al. 2009), decreased the cytotoxicity caused by MTX 1 and 5 μM in the NR uptake assay (Fig. 2B). However, 1-ABT did not cause a significant change in MTX-induced mitochondrial dysfunction (Fig. 2E).

To address the role of metabolism in MTX cytotoxicity, DAS (50 μM), a CYP2E1 inhibitor (Jin et al. 2013), was used in both cytotoxicity assays, without causing any meaningful changes regarding the effects caused by MTX (Fig. 2C,F).

Phenobarbital increased the cytotoxicity caused by MTX in differentiated AC16 cells when assessed by the neutral red uptake assay

The effects of the CYP2B6 inducer (Deng et al. 2013; Lin 2006) and aldo–keto reductases inhibitor (Behnia and Boroujerdi 1999), PHB, at 1 mM was evaluated through the

MTT reduction and NR uptake assays (Fig. 3A, C). In the NR uptake assay, PHB increased the cytotoxicity elicited by MTX 1 or 5 μM at 48 h, as can be seen in Fig. 3A. In the MTT assay, PHB did not cause meaningful changes in the MTX-induced cytotoxicity at 48 h (Fig. 3C). The use of PHB at 1 mM *per se* did not cause any toxicity when compared to control cells in both cytotoxicity tests performed. RIF (10 μM), a strong inducer of metabolizing enzymes such as CYP3A4 (Lin 2006), was not able to significantly change the MTX-elicited cytotoxicity at 48 h (Fig. 3B, D), in both assays.

Naphthoquinoxaline caused mitochondrial dysfunction in differentiated AC16 cells

Since some of CYP450 modulators altered MTX-induced cytotoxicity, and because among the known MTX metabolites only the NAPHT is commercially available, we next pursued to investigate the cytotoxicity profile of NAPHT (1 to 10 μM) on differentiated AC16 cells. Regarding the NR uptake assay, no meaningful differences were seen at all tested concentrations (Fig. 4A). On the other hand, the results showed that NAPHT caused a
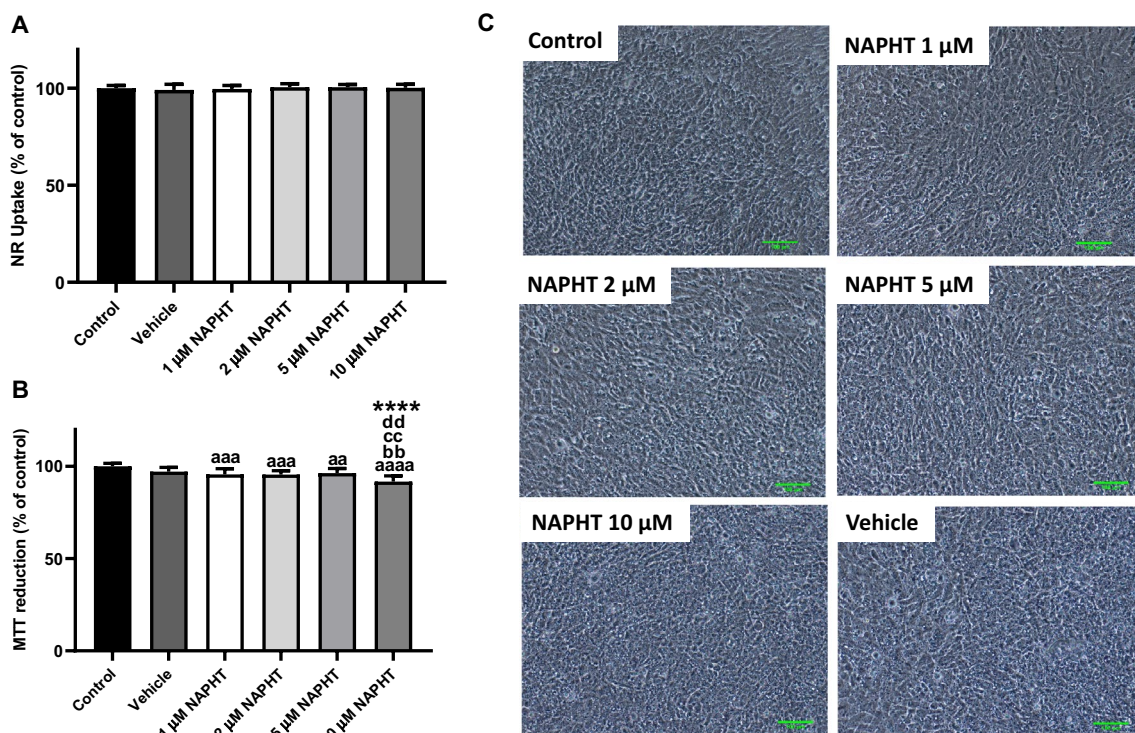
Fig. 4 Lysosomal and mitochondrial dysfunction were evaluated by the NR uptake (**A**) and the MTT reduction (**B**) assays, respectively. **A, B** differentiated AC16 cells incubated with 1, 2, 5, or 10 μM of naphthoquinoxaline (NAPHT) for 48 h. Results are presented as mean ± SD of 3 independent experiments (total of 12 wells). The statistical analyses were performed using the Kruskal–Wallis test, followed by the Dunn's post hoc test in the NR uptake assay and one-way ANOVA test, followed by the Sidak's post hoc test for the

MTT reduction assay ($^{aa}p < 0.01$, $^{aaa}p < 0.001$, $^{aaaa}p < 0.0001$ *versus* control; $^{bb}p < 0.01$ *versus* 1 μM; $^{cc}p < 0.01$ *versus* 2 μM; $^{dd}p < 0.001$ *versus* 5 μM; $^{****}p < 0.05$ *versus* vehicle). DMSO (final concentration of 0.1% *v/v*) was used as vehicle. **C** Phase-contrast microphotographs of differentiated AC16 cells after a 48-h incubation. Images are representative of three independent experiments (scale bar represents 100 μm)
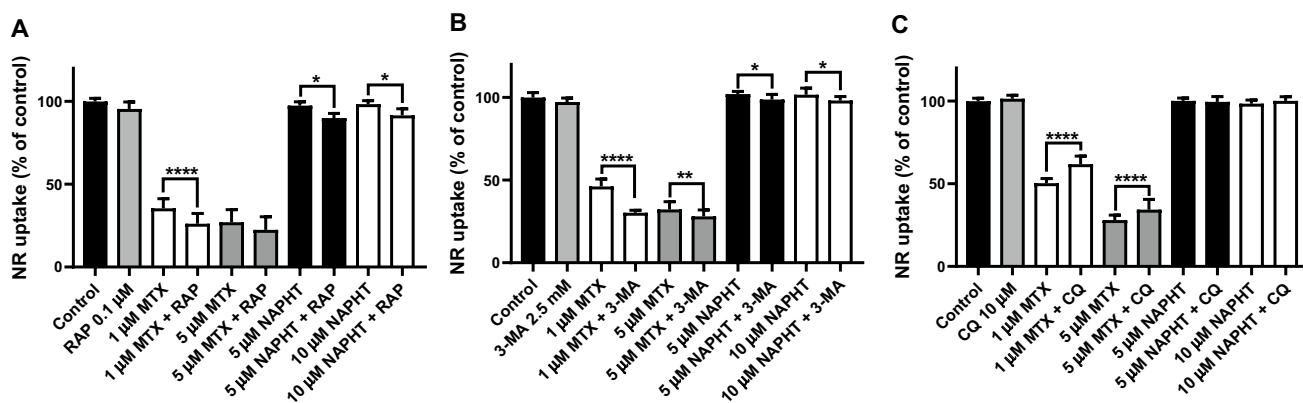

Fig. 5 Lysosomal dysfunction was evaluated by the NR uptake assay in differentiated AC16 cells incubated with 1 or 5 μM of MTX or 5 or 10 μM of NAPHT for 48 h with or without: **A** rapamycin (RAP) (0.1 μM final concentration) or **B** 3-methyladenine (3-MA) (2.5 mM final concentration) or **C** chloroquine (CQ) (10 μM final concentra-

tion). Results are presented as mean ± SD of 3 independent experiments (total of 12 wells). The statistical analyses performed was the Kruskal–Wallis test, followed by the Dunn's post hoc test ($^*p < 0.05$, $^{**}p < 0.01$, $^{****}p < 0.0001$, MTX or NAPHT *versus* MTX or NAPHT + 3-MA or CQ or RAP)

concentration-dependent cytotoxicity in the MTT assay (Fig. 4B) at 48 h. In MTT reduction assay, the values were, in the following conditions and in percentage: 1 µM: $95.16 \pm 2.28\%$, 2 µM: $95.51 \pm 2.14\%$, 5 µM: $96.37 \pm 2.44\%$, and 10 µM: $91.73 \pm 3.11\%$, when compared to control cells ($100.00 \pm 1.62\%$) and vehicle ($97.16 \pm 2.28\%$) (Fig. 4B). Phase-contrast microscopy did not reveal any important changes in cells' morphology (Fig. 4C) after incubation with NAPHT (1 to 10 µM).

In the Hoechst staining, no nuclear condensation was seen in any of the conditions evaluated (Figure S3). Ethidium bromide/acridine orange staining was also used to evaluate

the NAPHT effects on differentiated AC16 cells. Vehicle incubated differentiated AC16 cells showed a regular-sized fluorescent green nucleus and the NAPHT-incubated cells showed green nucleus (Figure S4).

Induction of autophagy exacerbated the cytotoxicity of mitoxantrone in differentiated AC16 cells

After assessing the cytotoxic effects of both MTX and NAPHT and since the assay indirectly evaluating lysosome functionality (the NR uptake assay) showed some

Fig. 6 **LC3B-II** (16 kDa) and **LC3B-I** (18 kDa) expression evaluated by western blotting, from differentiated AC16 cells incubated with MTX or NAPHT for 48 h. Values are expressed as ratio of optic density of LC3B-II or LC3B-I to GAPDH or ratio of LC3B-II to LC3B-I and as mean $\pm$ SD. They were obtained from 3 (2 wells per experiment, total of 6 wells *per* condition) independent experiments. Statistical comparisons were made using the one-way ANOVA test, followed by the Sidak post hoc test to compare with the control group: *$p <$ 0.05; ***$p <$ 0.001; ****$p <$ 0.0001 *versus* control. Protein loading was confirmed by GAPDH levels
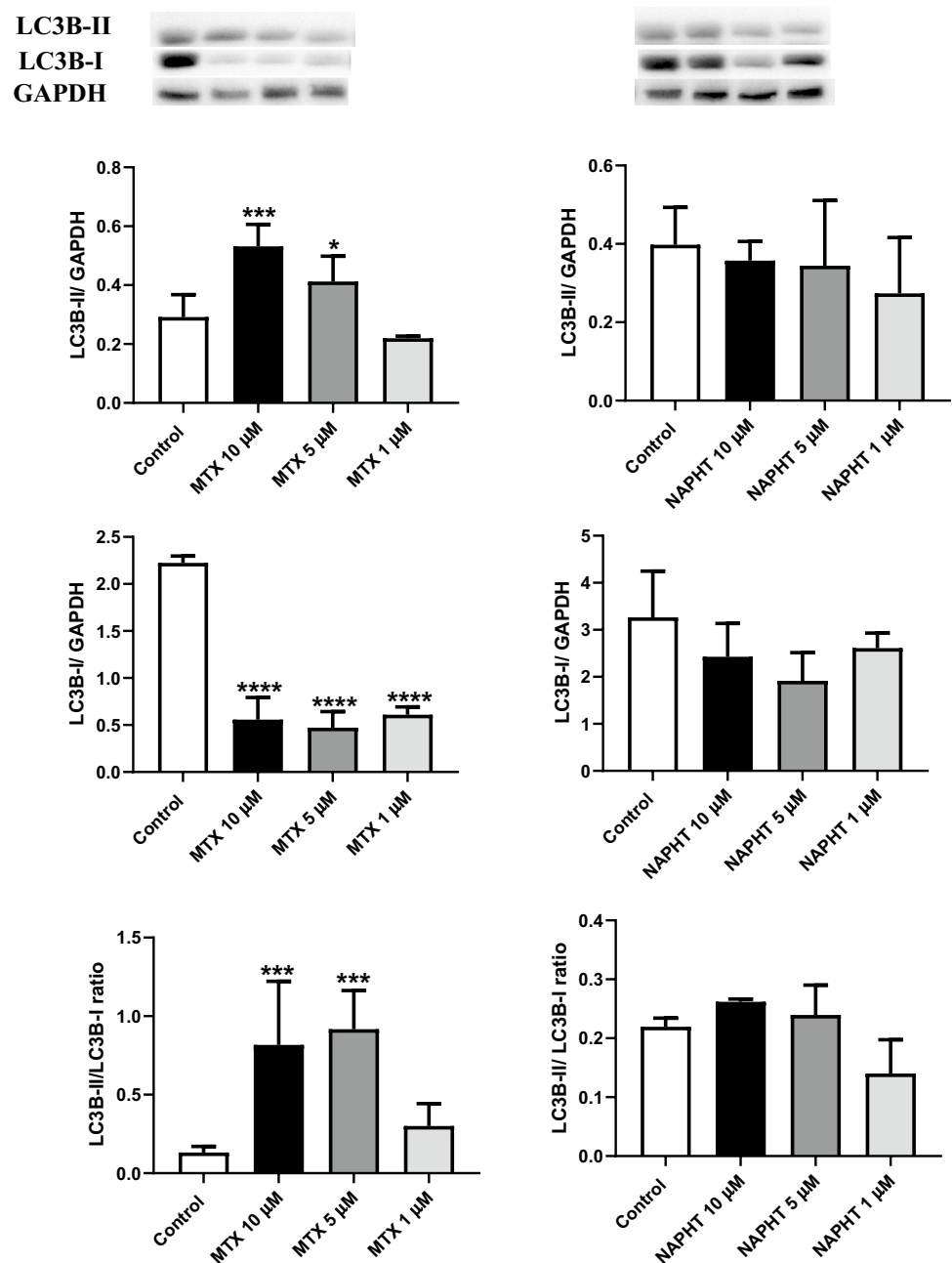
changes when addressing the CYP450 modulators, namely 1-ABT, MTP and PHB, autophagy was next investigated. RAP, 3-MA, and CQ, classic autophagic modulators, act on different stages of autophagy. RAP is an inhibitor of the mTORC1 receptor that can bind to the receptor and then activate autophagy acting on the mTOR pathway (Sarkar et al. 2009). At 48 h, the incubation with RAP exacerbated the cytotoxicity caused by MTX and NAPHT assessed by the NR uptake assay (Fig. 5A). Instead, phagophore formation and the nucleation of the autophagosome in autophagy require class III phosphatidylinositol 3-kinase (PI3K-III), which can be blunted by PI3K inhibitors (Baek et al. 2012). 3-MA is an inhibitor of PI3K-III, which is located upstream of the IGF/PI3K/mTOR/ULK pathway. At 48 h, the treatment with 3-MA exacerbated the cytotoxicity caused by MTX and NAPHT (Fig. 5B). Further along the way of autophagy, CQ mainly blocks autophagy by impairing autophagosome fusion with lysosomes (Mauthe et al. 2018), and prejudicing the autophagic flux. Herein, late-stage autophagy-blocker CQ (10 μM) partially reduced the cytotoxicity of MTX towards differentiated AC16 cells (Fig. 5C), while not causing any meaningful changes towards NAPHT exposed cells. The incubation with 3-MA at 2.5 mM, RAP at 0.1 μM, and CQ 10 μM per

se did not cause any significant toxicity when compared to control cells (Fig. 5).

Mitoxantrone initiated the autophagic process in differentiated AC16 cells

The expression of autophagy-related proteins was assessed by western blot after differentiated AC16 cells exposure to MTX or NAPHT for 48 h. Microtubule-associated protein 1A/1B-light chain 3 (LC3) is a soluble protein involved in autophagy. During this process, the cytosolic form of LC3 (LC3-I) is conjugated to phosphatidylethanolamine to form LC3 phosphatidylethanolamine conjugate (LC3-II), which is recruited into autophagosomal membranes. When autophagosomes fuse with lysosomes to form autolysosomes, intra-autophagosomal components, namely LC3-II, are degraded by lysosomal hydrolases (Tanida et al. 2008). The western blot analysis demonstrated that 10 and 5 μM MTX increased the levels of LC3B-II and induced the conversion of LC3B-I to LC3B-II (Fig. 6), causing a decrease in the protein expression of LC3B-I. These results confirm that MTX exposure can promote the synthesis of autophagosomes in differentiated AC16 cells. On the other hand, in cells exposed to NAPHT, no

Fig. 7 p62 (62 kDa) and **beclin-1** (60 kDa) expression evaluated by western blotting, from differentiated AC16 cells incubated with MTX or NAPHT. Results are presented ratio of optic density (OD) of p62/Beclin1 over OD of GAPDH and as mean ± SD of 3 independent experiments (2 wells per experiment, total of 6 wells per condition). Statistical comparisons were made using the one-way ANOVA test, followed by the Sidak post hoc test to compare with the control group: *$p <$ 0.05; **$p <$ 0.01; ***$p <$ 0.001; ****$p <$ 0.0001 *versus* control. Protein loading was confirmed by GAPDH levels
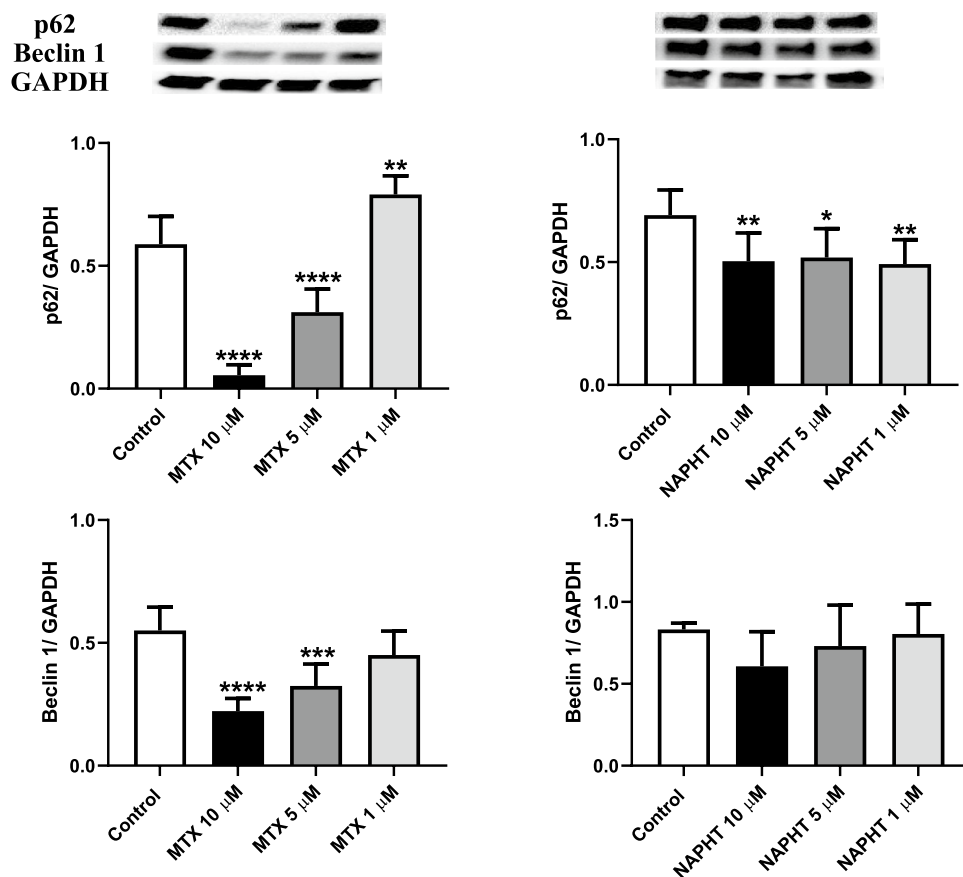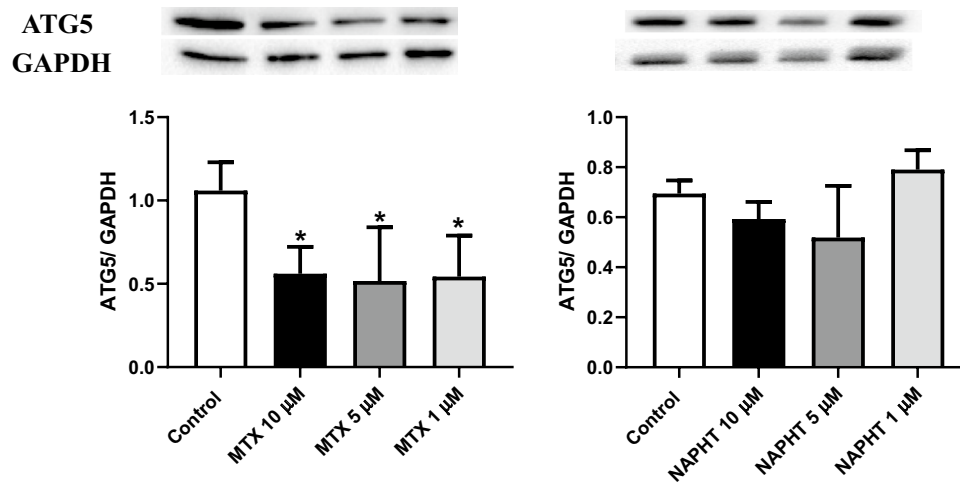
Fig. 8 ATG5 (50 kDa) expression was evaluated by western blotting, in differentiated AC16 cells incubated with 1, 5, or 10 μM of MTX or NAPHT for 48 h. Results are presented as ratio of optic density (OD) of ATG5 to OD of GAPDH and as mean ± SD of 3 independent experiments (2 wells per experiment, total of 6 wells per condition). Statistical comparisons were made using the one-way ANOVA test, followed by the Sidak post hoc test to compare with the control group: *$p < 0.05$ *versus* control. Protein loading was confirmed by GAPDH levels

significant changes in LC3-II or LC3-I were observed when compared to the control cells (Fig. 6).

Mitoxantrone and its metabolite inhibited the beclin-1 related autophagic response while promoting the p62-related autophagosome formation

p62 Protein, also called sequestosome 1 (SQSTM1) is rapidly degraded during autophagy and may be used as a marker to study the autophagic flux (Bjørkøy et al. 2009); the analysis of its intracellular levels was performed by western blot 48 h after MTX or NAPHT. As Fig. 7 shows, a significant decrease in p62 was detected for 10 and 5 μM MTX, while a slight but significant increase was observed for 1 μM MTX. The downregulation of p62 was detected in NAPHT-incubated cells when compared with control, indicating activation of the autophagic flux.

Beclin-1 forms a multimeric complex with vacuolar protein sorting 34 and class III PI3K, which is necessary for the formation of autophagosome, being, therefore, an essential mediator of autophagy (Mizushima 2007). A significant decrease in Beclin-1 expression was observed in the MTX-incubated cells at 10 and 5 μM concentrations compared with control, while no differences were observed in differentiated AC16 cells exposed to NAPHT (Fig. 8).

Mitoxantrone caused downregulation of ATG5

ATG5 plays a role in the elongation of the phagophore and its subsequent maturation into the complete autophagosome

(Galluzzi et al. 2017). The western blot analysis demonstrated that MTX significantly decreased the levels of ATG5 in the differentiated AC16 cells, while no changes were observed after NAPHT (Fig. 7).

Discussion

This work represents an unprecedented broad study on the cytotoxicity of MTX and its' metabolite NAPHT in differentiated human AC16 cells. Extensive concentration-dependent cytotoxicity caused by MTX affected mitochondrial function and lysosome uptake, being that the MTT assay was the most sensitive assay. In previous works, MTX was also shown to be toxic to differentiated (Reis-Mendes et al. 2017) and undifferentiated H9c2 myoblasts (Kluza et al. 2004; Rossato et al. 2013b). No clear signs of late apoptosis were observed in differentiated AC16 cells when evaluated by Hoechst, but in ethidium bromide/acridine staining some condensed nuclei appeared. Signs of apoptosis were previously reported after MTX in undifferentiated H9c2 cells and in the breast cancer cell line MTLn3 (Kluza et al. 2004), as well as in HL-1 cardiac cells (Costa et al. 2020).

Since other studies have hinted that metabolism could be partly responsible for MTX-induced cytotoxicity, both in cardiac models (H9c2 cells) (Rossato et al. 2013a) and in hepatic models (HepG2 cells and cultured rat hepatocytes) (Duthie and Grant 1989; Mewes et al. 1993), we studied the putative action of different metabolism modulators, to understand whether metabolism had any role on MTX-induced cardiotoxicity in a human in vitro model. At this

point, we have no information on AC16 cell line metabolic characteristics, so we could only rely on the scarce data available in the literature regarding MTX metabolism. In our study, the inhibition of CYP450-mediated metabolism by MTP significantly increased MTX-induced cytotoxicity, contradicting previous studies, where MTP showed to prevent the cytotoxic effect of MTX in human liver-derived HepG2 hepatoma cells (Duthie and Grant 1989; Mewes et al. 1993), cultured rat hepatocytes model (Mewes et al. 1993), and MCF-7 human breast cancer cells (Li et al. 1995). Rossato et al. demonstrated partial protection towards MTX cytotoxicity (100 nM and 1 μM) in rat H9c2 undifferentiated cells at 96 h, after the pre-incubation with MTP or with DAS (Rossato et al. 2013a). However, in the present work with differentiated human AC16 cells, DAS did not revert the cytotoxicity caused by MTX, showing species variability or even cell line specificities. Previous studies hypothesize that MTX produces reactive intermediates when it is metabolized by the CYP2E1 enzyme system (Feofanov et al. 1997a; Rossato et al. 2013a). Although CYP2E1 is abundant in the heart (Michaud et al. 2010) and an upregulated CYP2E1 has multiple cardiac pathophysiological roles, including increased oxidative stress and apoptosis, as well as energy supply to meet the energy demand of the heart in certain disease states (Guan et al. 2019), we did not found this isoenzyme to have any particular importance towards of MTX cytotoxicity. Another important finding of this work is the partial protection obtained with pre-incubation with 1-ABT, a suicide nonspecific CYP450 inhibitor (de Montellano 2018) against MTX-induced cytotoxicity. This result suggests that CYP450 metabolism has a small relevance in MTX cytotoxicity in our experimental model, but there is an apparent contradiction to the results obtained in MPT. 1-ABT does not allow competition with the substrates, in this case MTX, because it destroys the enzymes; moreover, it has been proven that 1-ABT interferes with the activity of other enzymes (Sun et al. 2011), while MPT interferes with other key pathways for the heart (Blättler et al. 2007; Wright et al. 1996), which may explain the differences seen.

We also studied the role of two metabolism inducers, RIF and PHB. RIF efficiently induces human CYP3A4, whereas CYP2B6 and CYP2C9 are also induced by RIF, but to a lesser extent (Handschin and Meyer 2003; Lin 2006). In the present study, RIF did not significantly change the MTX-induced cytotoxicity in the differentiated AC16 cells, when co-incubated with MTX. Concerning PHB, it is a potent inducer of human CYP2B6, and, to a lesser extent, it induces human CYP2C9 and CYP3A4 (Handschin and Meyer 2003; Lin 2006). In this work, PHB exacerbated the cytotoxicity caused by MTX when evaluated by the NR uptake assay, when co-incubated for 48 h. Similarly, Li et al. observed that PHB potentiates the MTX cytotoxicity in MCF-7 human breast cancer cells (Li et al. 1995). PHB increases

CYP activity and MTX may be oxidized to form reactive intermediaries (Kolodziejczyk et al. 1988; Wolf et al. 1986). However, one should keep in mind that PHB is also an inhibitor of cytosolic aldo–keto reductases (Kawalek and Gilbertson 1976). Additionally, the major metabolic pathway of anthracyclines is the reduction to C13-hydroxy metabolites, which is mediated by a group of NADPH-dependent carbonyl reducing enzymes belonging to short-chain dehydrogenase/reductase and aldo–keto reductase superfamilies (Bains et al. 2010; Kassner et al. 2008). Such alcohol anthracycline metabolites may cause cardiotoxicity due to their accumulation in cardiac tissue (Menna et al. 2007), when produced *in loco*. Since MTX is highly resistant to reductive metabolism due to its large negative reduction potential (Evison et al. 2016), we believe that PHB acts more as an inducer of MTX oxidation upon its action on P450 enzymes expression. As stated, MTX is more susceptible to enzymatically driven oxidation, which may generate intermediates with the potential for reaction with intracellular nucleophiles and engage in the drugs' cytotoxicity (Evison et al. 2016), exacerbating it. Moreover, the heart is very sensitive to oxidative stress because of its high metabolic activity and low antioxidant defenses (Costa et al. 2013), making it a target for those reactive compounds.

The NAPHT metabolite originates from oxidative action of cellular enzymes (Blanz et al. 1991b; Kolodziejczyk et al. 1988; Wolf et al. 1986). Considering the interspecies variability, the mono- and dicarboxylic acid derivatives of MTX are major by-products of human metabolism, while in rats NAPHT is the main metabolite (Blanz et al. 1991b; Richard et al. 1991). NAPHT has been described as the product of MTX metabolism through systems containing CYP450 enzymes and peroxidases and it has been found in urine of humans treated with MTX (Blanz et al. 1991b; Brück and Brück 2011), advocating for its importance both in the clinical effects of MTX but also in its' putative toxicity. In vitro, when given at similar concentrations as MTX, NAPHT caused significant but smaller disruption of the MTT reduction ability and it did not affect lysosomes in differentiated AC16 cells. MTX has been described as drug that accumulates in lysosomes, which can explain these differences (Evison et al. 2016). The lower cytotoxicity of NAPHT compared with MTX when using equimolar concentrations was corroborated by our group in a previous work with a different cellular model (differentiated H9c2 cells) (Reis-Mendes et al. 2017). Moreover, Shipp et al. in isolated neonatal rat heart myocytes exposed to MTX/NAPHT for 3 h (followed by a 72-h free drug period) observed that the metabolite also elicited lower cytotoxicity to myocytes when compared with MTX (Shipp et al. 1993). Altogether, NAPHT is not the major contributor to MTX toxicity as seen by its lower cytotoxicity and by the residual influence of inhibitors/inducers on the observed MTX cytotoxicity even when given in

considerable amounts. However, some aspects cannot be neglected when analyzing this drug/metabolite duo. Perhaps the poor ability of NAPHT to enter cardiac cells when given/produced exogenously makes us assume that it does not contribute largely to the MTX cardiotoxicity. Nevertheless, it has been described that intermediaries seen in the formation of NAPHT may be reactive (Kolodziejczyk et al. 1988) and may cause toxicity, which can explain the higher toxicity of MTX, when PHB is present. Then again, as the ratio of metabolites in humans and experimental animals is dissimilar, pending on NAPHT in experimental animals, and as both humans and experimental animals show clear signs of cumulative dose dependent cardiotoxicity (Dores-Sousa et al. 2015; Evison et al. 2016; Li et al. 1995; Reis-Mendes et al. 2021; Scott and Figgitt 2004), that per se is a strong point showing that MTX metabolism is not a key factor to the reported heart damage.

Autophagy and apoptosis are key processes for cardiac homeostasis. Autophagy is a cellular pathway that regulates the transport of cytoplasmic macromolecules and organelles to lysosomes for degradation (Galluzzi et al. 2017). Autophagy comprises several steps, sequestration, transport to lysosomes, degradation, and use of degradation products (Mizushima 2007). Autophagy serves a protective response to most anticancer drugs and in the pathogenesis process (Chen et al. 2013; Nakai et al. 2007), but it can be modulated at different stages, being that many drugs act by dissimilar mechanisms (Liao et al. 2019). The most used inducer of autophagy is RAP, which activates autophagy by inhibiting mTORC1, a negative regulator of autophagy (Liao et al. 2019). In this work, RAP exacerbated the cytotoxicity caused by MTX and NAPHT when evaluated by the NR uptake assay. As far as we know, this was the first study in cardiac models with MTX, NAPHT and mTOR inhibitors, showing that macroautophagy induction increases MTX and its metabolite toxicity. In addition, Guan et al. showed that combining mTOR inhibitors and MTX has synergistic cytotoxic effects against breast cancer cells in vitro (MCF-7 and MDA-MB-231 cells) and in vivo (MDA-MB-231 cells with or without silencing eEF-2 K were injected subcutaneously into 6-week-old female nude mice) (Guan et al. 2020). Therefore, although inhibitors of mTOR could be interesting to increase anticancer therapy efficacy, they can also contribute to MTX cardiotoxicity and caution is required.

In other steps of autophagy, at an early stage, the autophagy inhibitor 3-MA can suppress autophagy by inhibiting phosphatidylinositol 3-kinase, class III, PI3K-III (Liao et al. 2019). In this work, 3-MA exacerbated the cytotoxicity caused by MTX and NAPHT evaluated by the NR uptake assay. In another study, using differentiated H9c2 cells, 3-MA caused a partial but meaningful reversion in toxicity caused by MTX and its metabolite NAPHT (Reis-Mendes et al. 2017), which seems to contradict the results

obtained herein. On the other hand, one cannot forget that PI3K-III and beclin-1 (discussed latter on) have tight and important roles, balancing both autophagy and apoptosis (Menon and Dhamija 2018), making the result analysis more complex. Following to another autophagy modulator, in this case at a later autophagy stage, CQ can prevent lysosomal acidification and block the degradation of autophagosomes and lysosomes (Liao et al. 2019). CQ partially reduced the MTX toxicity towards AC16 differentiated cells, showing that blocking autophagy at a later stage could be protective, whereas inducing it at earlier stages (with RAP) increases the damage inflicted.

There are studies that, despite not reporting the involvement of autophagy, demonstrate cytoplasmic vacuolization in the heart after MTX administration to mice (Dores-Sousa et al. 2015; Reis-Mendes et al. 2021), and in vitro in neonatal rat cardiomyocytes incubated to MTX (Shipp et al. 1993). In the present study, the upregulation of the autophagosome marker LC3-II and the downregulation of p62, which binds directly to LC3 and facilitates autophagosome degradation, were observed in MTX-treated differentiated AC16 cells, suggesting autophagy induction by MTX. The hallmark of autophagosome formation is characterized by the insertion of LC3-II within the inner and outer layers of the vesicle (Galluzzi et al. 2017). p62 expression does not affect autophagosome formation but influences protein aggregation and LC3-II formation, as silencing p62 activates autophagy through an increase in the conversion rate of LC3-I to LC3-II (Liu et al. 2016). p62 is a proteotoxic sensor able to bind to ubiquitylated misfolded proteins destined for clearance by autophagy and also to LC3, thereby targeting the autophagosome and facilitating clearance of ubiquitinated proteins (Su and Wang 2011). In a previous work of the group, we already described that proteasome was targeted by MTX (Costa et al. 2020), and therefore higher levels of misfolded proteins are expected, which may trigger this response. Conversely, Xie et al. demonstrated significant increase of LC3-II and downregulation of p62 in HepG2 cells exposed to MTX, suggesting that MTX treatment led to autophagy activation, which was further confirmed by the use of the lysosomal inhibitor CQ (Xie et al. 2020). Actually, Xie et al. showed that the exposure of HepG2 cells simultaneously to MTX and CQ enhanced the amount of LC3-II in comparison with exposure to only CQ, which confirmed the induction of autophagy by MTX (Xie et al. 2020). Also in cancer models, late-stage inhibition of autophagy by CQ, promoted apoptotic cell killing by MTX (Aguirre-Hernández et al. 2018). However, we observed that CQ decreased the cytotoxicity while preventing the maturation step of autophagy, revealing that other mechanisms are involved.

Beclin-1 is an autophagy-specific protein that regulates autophagosome formation and is therefore an essential mediator of autophagy (Mizushima 2007). Beclin-1

interacts with Bcl-2, which can result in inhibition of autophagy, but it also interacts with PI3K-III and can lead to upregulation of autophagy (Mizushima 2007). In this study, we observed a decrease in beclin-1 levels in the MTX-incubated differentiated AC16 cells at the concentration of 5 μM and 10 μM. No differences were observed in cells exposed to NAPHT. It appears that the increased autophagic flux seen by increased LC3-II and decreased p62 is not regulated by beclin-1, in strong opposition to what was seen in MTX-incubated HepG2 cells at the concentration of 5 μM and 7.5 μM (Xie et al. 2020). Nevertheless, the same work in HepG2 cells describes a slight decrease in beclin-1 at the MTX concentration of 10 μM (Xie et al. 2020). The decrease of beclin-1 that we observe in AC16 cells exposed to MTX may have two dual effects: decrease of autophagic flux via this route or increase apoptosis (Wirawan et al. 2010) induced by MTX, since the inhibition of PI3K-III further increases cytotoxicity.

Other routes involved in autophagy have been associated with the activity of two ubiquitin-like conjugation systems: (1) autophagy-related (ATG)7 and ATG10, which promote the conjugation of ATG5 to ATG12 in the context of a multiprotein complex containing ATG16L1; and (2) autophagy-related ATG3 and ATG7, which together with the ATG12-ATG5: ATG16L1 complex conjugates phosphatidylethanolamine to microtubule-associated protein 1 light chain 3 beta (LC3B) (Galluzzi et al. 2017). In our work, no changes in ATG5 levels in cells treated with NAPHT were observed when compared to the control. On the other hand, in cells incubated with MTX, we observed a significant decrease in ATG5 levels, when compared with control cells, showing that ATG5-dependent autophagy is also blunted after MTX. This result needs to be carefully looked, since MTX causes dose cumulative heart failure and a recent work showed that the loss of ATG5 causes changes in mitochondrial abundance and functionality and subtle but important alterations in subcellular calcium (Ljubojević-Holzer et al. 2021), all key players for a heathy heart.

Thus, MTX in AC16 cells leads to macroautophagy induction and elongation (seen by LC3-II increase and p62 decrease), but not by the beclin-1 and PI3K-III route. Inhibition of that route further increases cytotoxicity, possibly by activating apoptosis. On the other hand, ATG5 also decreases and as CQ reverts slightly MTX toxicity, we hypothesize that in this case autophagy is contributing to cell death.

In conclusion, conversion to NAPHT is not the major contributor to MTX toxicity elicited in differentiated AC16 cells, when given exogenously and therefore functioning as an extracardiac source of the metabolite. Even with the residual influence of inhibitors/inducers of metabolism on the MTX observed cytotoxicity, one cannot exclude it and it may result from the intermediaries that are appear during NAPHT formation (Kolodziejczyk et al. 1988). Moreover, MTX seems to act as an autophagy inducer possibly by a proteotoxic stimuli sensed by p62 and this autophagic flux possible contributes to MTX toxicity. Therefore, while the modulation of cardiotoxicity caused by MTX by metabolism seems residual, autophagy must be looked further to decrease the incidence of this life threatening adverse effect.

Declarations

Conflict of interest None.

References

Aguirre-Hernández C, Maya-Pineda H, Millán JS, Man YKS, Lu Y-J, Halldén G (2018) Sensitisation to mitoxantrone-induced apoptosis by the oncolytic adenovirus AdΔΔ through Bcl-2-dependent attenuation of autophagy. Oncogenesis 7(1):6

Alberts DS, Peng YM, Leigh S, Davis TP, Woodward DL (1985) Disposition of mitoxantrone in cancer patients. Cancer Res 45(4):1879–1884

An G, Morris ME (2010) HPLC analysis of mitoxantrone in mouse plasma and tissues: application in a pharmacokinetic study. J Pharm Biomed Anal 51(3):750–753

Baek KH, Park J, Shin I (2012) Autophagy-regulating small molecules and their therapeutic applications. Chem Soc Rev 41(8):3245–3263

Bains OS, Griglatti TA, Reid RE, Riggs KW (2010) Naturally occurring variants of human aldo-keto reductases with reduced in vitro metabolism of daunorubicin and doxorubicin. J Pharmacol Exp Ther 335(3):533–545

Behnia K, Boroujerdi M (1999) Inhibition of aldo-keto reductases by phenobarbital alters metabolism, pharmacokinetics and toxicity of doxorubicin in rats. J Pharm Pharmacol 51(11):1275–1282

Bik E, Mateuszuk L, Orleanska J, Baranska M, Chlopicki S, Majzner K (2021) Chloroquine-induced accumulation of autophagosomes and lipids in the endothelium. Int J Mol Sci 22:5

Bjørkøy G, Lamark T, Pankiv S, Øvervatn A, Brech A, Johansen T (2009) Monitoring autophagic degradation of p62/SQSTM1. Methods Enzymol 452:181–197

Blanz J, Mewes K, Ehninger G et al (1991a) Isolation and structure elucidation of urinary metabolites of mitoxantrone. Cancer Res 51(13):3427–3433

Blanz J, Mewes K, Ehninger G et al (1991b) Evidence for oxidative activation of mitoxantrone in human, pig, and rat. Drug Metab Dispos 19(5):871–880

Blättler SM, Rencurel F, Kaufmann MR, Meyer UA (2007) In the regulation of cytochrome P450 genes, phenobarbital targets LKB1 for necessary activation of AMP-activated protein kinase. Proc Natl Acad Sci U S A 104(3):1045–1050

Brück TB, Brück DW (2011) Oxidative metabolism of the anti-cancer agent mitoxantrone by horseradish, lacto-and lignin peroxidase. Biochimie 93(2):217–226

Bulutoglu B, Mert S, Rey-Bedón C, Deng SL, Yarmush ML, Usta OB (2019) Rapid maturation of the hepatic cell line Huh7 via CDK inhibition for PXR dependent CYP450 metabolism and induction. Sci Rep 9(1):15848

Chen ML, Yi L, Jin X et al (2013) Resveratrol attenuates vascular endothelial inflammation by inducing autophagy through the cAMP signaling pathway. Autophagy 9(12):2033–2045

Chiccarelli FS, Morrison JA, Cosulich DB et al (1986) Identification of human urinary mitoxantrone metabolites. Cancer Res 46(9):4858–4861

Costa VM, Carvalho F, Duarte JA, Bastos ML, Remião F (2013) The heart as a target for xenobiotic toxicity: the cardiac susceptibility to oxidative stress. Chem Res Toxicol 26(9):1285–1311

Costa VM, Capela JP, Sousa JR et al (2020) Mitoxantrone impairs proteasome activity and prompts early energetic and proteomic changes in HL-1 cardiomyocytes at clinically relevant concentrations. Arch Toxicol 94(12):4067–4084

Cuervo AM (2004) Autophagy: many paths to the same end. Mol Cell Biochem 263(1–2):55–72

Davidson MM, Nesti C, Palenzuela L et al (2005) Novel cell lines derived from adult human ventricular cardiomyocytes. J Mol Cell Cardiol 39(1):133–147

De Meyer GR, Martinet W (2009) Autophagy in the cardiovascular system. Biochim Biophys Acta 1793(9):1485–1495

de Montellano PRO (2018) 1-Aminobenzotriazole: a mechanism-based cytochrome P450 inhibitor and probe of cytochrome P450 biology. Med Chem 8:3

Deng Y, Wang L, Yang Y et al (2013) In vitro inhibition and induction of human liver cytochrome P450 enzymes by gentiopicroside: potent effect on CYP2A6. Drug Metab Pharmacokinet 28(4):339–344

Dionísio F, Araújo AM, Duarte-Araújo M et al (2022) Cardiotoxicity of cyclophosphamide's metabolites: an in vitro metabolomics approach in AC16 human cardiomyocytes. Arch Toxicol 96(2):653–671

Dores-Sousa JL, Duarte JA, Seabra V, Bastos ML, Carvalho F, Costa VM (2015) The age factor for mitoxantrone's cardiotoxicity: multiple doses render the adult mouse heart more susceptible to injury. Toxicology 329:106–119

Duthie SJ, Grant MH (1989) The role of reductive and oxidative metabolism in the toxicity of mitoxantrone, adriamycin and menadione in human liver derived Hep G2 hepatoma cells. Br J Cancer 60(4):566–571

Ehninger G, Schuler U, Proksch B, Zeller KP, Blanz J (1990) Pharmacokinetics and metabolism of mitoxantrone A Review. Clin Pharmacokinet 18(5):365–380

Evison BJ, Sleebs BE, Watson KG, Phillips DR, Cutts SM (2016) Mitoxantrone, more than just another topoisomerase II poison. Med Res Rev 36(2):248–299

Feofanov A, Sharonov S, Fleury F, Kudelina I, Nabiev I (1997a) Quantitative confocal spectral imaging analysis of mitoxantrone within living K562 cells: intracellular accumulation and distribution of monomers, aggregates, naphtoquinoxaline metabolite, and drug-target complexes. Biophys J 73(6):3328–3336

Feofanov A, Sharonov S, Kudelina I, Fleury F, Nabiev I (1997b) Localization and molecular interactions of mitoxantrone within living K562 cells as probed by confocal spectral imaging analysis. Biophys J 73(6):3317–3327

Fox EJ (2004) Mechanism of action of mitoxantrone. Neurology 63(12 Suppl 6):S15–S18

Galluzzi L, Baehrecke EH, Ballabio A et al (2017) Molecular definitions of autophagy and related processes. Embo j 36(13):1811–1836

Guan F, Yang X, Li J et al (2019) New molecular mechanism underlying myc-mediated cytochrome P450 2E1 upregulation in apoptosis and energy metabolism in the myocardium. J Am Heart Assoc 8(1):e009871

Guan Y, Jiang S, Ye W et al (2020) Combined treatment of mitoxantrone sensitizes breast cancer cells to rapalogs through blocking eEF-2K-mediated activation of Akt and autophagy. Cell Death Dis 11(11):948

Handschin C, Meyer UA (2003) Induction of drug metabolism: the role of nuclear receptors. Pharmacol Rev 55(4):649–673

Hariharan N, Zhai P, Sadoshima J (2011) Oxidative stress stimulates autophagic flux during ischemia/reperfusion. Antioxid Redox Signal 14(11):2179–2190

Ikeda S, Zablocki D, Sadoshima J (2022) The role of autophagy in death of cardiomyocytes. J Mol Cell Cardiol 165:1–8

Jin M, Ande A, Kumar A, Kumar S (2013) Regulation of cytochrome P450 2e1 expression by ethanol: role of oxidative stress-mediated pkc/jnk/sp1 pathway. Cell Death Dis 4(3):e554

Kassner N, Huse K, Martin HJ et al (2008) Carbonyl reductase 1 is a predominant doxorubicin reductase in the human liver. Drug Metab Dispos 36(10):2113–2120

Kawalek JC, Gilbertson JR (1976) Partial purification of the NADPH-dependent aldehyde reductase from bovine cardiac muscle. Arch Biochem Biophys 173(2):649–657

Kluza J, Marchetti P, Gallego MA et al (2004) Mitochondrial proliferation during apoptosis induced by anticancer agents: effects of doxorubicin and mitoxantrone on cancer and cardiac cells. Oncogene 23(42):7018–7030

Kolodziejczyk P, Reszka K, Lown JW (1988) Enzymatic oxidative activation and transformation of the antitumor agent mitoxantrone. Free Radic Biol Med 5(1):13–25

Kostin S, Pool L, Elsässer A et al (2003) Myocytes die by multiple mechanisms in failing human hearts. Circ Res 92(7):715–724

Li SJ, Rodgers EH, Grant MH (1995) The activity of xenobiotic enzymes and the cytotoxicity of mitoxantrone in MCF 7 human breast cancer cells treated with inducing agents. Chem Biol Interact 97(2):101–118

Liao YX, Yu HY, Lv JY et al (2019) Targeting autophagy is a promising therapeutic strategy to overcome chemoresistance and reduce metastasis in osteosarcoma. Int J Oncol 55(6):1213–1222

Lin JH (2006) CYP induction-mediated drug interactions: in vitro assessment and clinical implications. Pharm Res 23(6):1089–1116

Linder CD, Renaud NA, Hutzler JM (2009) Is 1-aminobenzotriazole an appropriate in vitro tool as a nonspecific cytochrome P450 inactivator? Drug Metab Dispos 37(1):10–13

Liu WJ, Ye L, Huang WF et al (2016) p62 links the autophagy pathway and the ubiqutin-proteasome system upon ubiquitinated protein degradation. Cell Mol Biol Lett 21:29

Ljubojević-Holzer S, Kraler S, Djalinac N et al (2021) Loss of autophagy protein ATG5 impairs cardiac capacity in mice and humans through diminishing mitochondrial abundance and disrupting Ca2+ cycling. Cardiovasc Res 118(6):1492–1505

Mauthe M, Orhon I, Rocchi C et al (2018) Chloroquine inhibits autophagic flux by decreasing autophagosome-lysosome fusion. Autophagy 14(8):1435–1455

McGahon AJ et al (1995) The end of the (cell) line: methods for the study of apoptosis in vitro. In: Schwartz LW, Osborne BA (eds) methods in cell biology, vol 46. Academic Press, New York, pp 153–185

Menna P, Minotti G, Salvatorelli E (2007) In vitro modeling of the structure-activity determinants of anthracycline cardiotoxicity. Cell Biol Toxicol 23(1):49–62

Menon MB, Dhamija S (2018) Beclin 1 phosphorylation—at the center of autophagy regulation. Front Cell Dev Biol 6:137

Mewes K, Blanz J, Ehninger G, Gebhardt R, Zeller KP (1993) Cytochrome P-450-induced cytotoxicity of mitoxantrone by formation of electrophilic intermediates. Cancer Res 53(21):5135–5142

Michaud V, Frappier M, Dumas MC, Turgeon J (2010) Metabolic activity and mRNA levels of human cardiac CYP450s involved in drug metabolism. PLoS ONE 5(12):e15666

Mizushima N (2007) Autophagy: process and function. Genes Dev 21(22):2861–2873

Nakai A, Yamaguchi O, Takeda T et al (2007) The role of autophagy in cardiomyocytes in the basal state and in response to hemodynamic stress. Nat Med 13(5):619–624

Panousis C, Kettle AJ, Phillips DR (1994) Oxidative metabolism of mitoxantrone by the human neutrophil enzyme myeloperoxidase. Biochem Pharmacol 48(12):2223–2230

Panousis C, Kettle AJ, Phillips DR (1997) Neutrophil-mediated activation of mitoxantrone to metabolites which form adducts with DNA. Cancer Lett 113(1–2):173–178

Parzych KR, Klionsky DJ (2014) An overview of autophagy: morphology, mechanism, and regulation. Antioxid Redox Signal 20(3):460–473

Reis-Mendes AF, Sousa E, de Lourdes BM, Costa VM (2015) The role of the metabolism of anticancer drugs in their induced-cardiotoxicity. Curr Drug Metab 17(1):75–90

Reis-Mendes A, Gomes AS, Carvalho RA et al (2017) Naphthoquinoxaline metabolite of mitoxantrone is less cardiotoxic than the parent compound and it can be a more cardiosafe drug in anticancer therapy. Arch Toxicol 91(4):1871–1890

Reis-Mendes A, Dores-Sousa JL, Padrão AI et al (2021) Inflammation as a possible trigger for mitoxantrone-induced cardiotoxicity: an in vivo study in adult and infant mice. Pharmaceuticals 14:6

Repetto G, del Peso A, Zurita JL (2008) Neutral red uptake assay for the estimation of cell viability/cytotoxicity. Nat Protoc 3(7):1125–1131

Richard B, Fabre G, De Sousa G, Fabre I, Rahmani R, Cano JP (1991) Interspecies variability in mitoxantrone metabolism using primary cultures of hepatocytes isolated from rat, rabbit and humans. Biochem Pharmacol 41(2):255–262

Rossato LG, Costa VM, de Pinho PG et al (2013a) The metabolic profile of mitoxantrone and its relation with mitoxantrone-induced cardiotoxicity. Arch Toxicol 87(10):1809–1820

Rossato LG, Costa VM, Vilas-Boas V et al (2013b) Therapeutic concentrations of mitoxantrone elicit energetic imbalance in H9c2 cells as an earlier event. Cardiovasc Toxicol 13(4):413–425

Sampath-Kumar R, Yu M, Khalil MW, Yang K (1997) Metyrapone is a competitive inhibitor of 11beta-hydroxysteroid dehydrogenase type 1 reductase. J Steroid Biochem Mol Biol 62(2–3):195–199

Sarkar S, Ravikumar B, Floto RA, Rubinsztein DC (2009) Rapamycin and mTOR-independent autophagy inducers ameliorate toxicity of polyglutamine-expanded huntingtin and related proteinopathies. Cell Death Differ 16(1):46–56

Scott LJ, Figgitt DP (2004) Mitoxantrone: a review of its use in multiple sclerosis. CNS Drugs 18(6):379–396

Shipp NG, Dorr RT, Alberts DS, Dawson BV, Hendrix M (1993) Characterization of experimental mitoxantrone cardiotoxicity and its partial inhibition by ICRF-187 in cultured neonatal rat heart cells. Cancer Res 53(3):550–556

Soares AS, Costa VM, Diniz C, Fresco P (2014) Combination of Cl-IB-MECA with paclitaxel is a highly effective cytotoxic therapy causing mTOR-dependent autophagy and mitotic catastrophe on human melanoma cells. J Cancer Res Clin Oncol 140(6):921–935

Su H, Wang X (2011) p62 Stages an interplay between the ubiquitin-proteasome system and autophagy in the heart of defense against proteotoxic stress. Trends Cardiovasc Med 21(8):224–228

Sun Q, Harper TW, Dierks EA et al (2011) 1-Aminobenzotriazole, a known cytochrome P450 inhibitor, is a substrate and inhibitor of N-acetyltransferase. Drug Metab Dispos 39(9):1674–1679

Takemura G, Miyata S, Kawase Y, Okada H, Maruyama R, Fujiwara H (2006) Autophagic degeneration and death of cardiomyocytes in heart failure. Autophagy 2(3):212–214

Tanida I, Ueno T, Kominami E (2008) LC3 and autophagy. Methods Mol Biol 445:77–88

Valentim L, Laurence KM, Townsend PA et al (2006) Urocortin inhibits Beclin1-mediated autophagic cell death in cardiac myocytes exposed to ischaemia/reperfusion injury. J Mol Cell Cardiol 40(6):846–852

Wirawan E, Vande Walle L, Kersse K et al (2010) Caspase-mediated cleavage of Beclin-1 inactivates Beclin-1-induced autophagy and enhances apoptosis by promoting the release of proapoptotic factors from mitochondria. Cell Death Dis 1(1):e18–e18

Wolf CR, Macpherson JS, Smyth JF (1986) Evidence for the metabolism of mitozantrone by microsomal glutathione transferases and 3-methylcholanthrene-inducible glucuronosyl transferases. Biochem Pharmacol 35(9):1577–1581

Wormhoudt LW, Commandeur JN, Vermeulen NP (1999) Genetic polymorphisms of human N-acetyltransferase, cytochrome P450, glutathione-S-transferase, and epoxide hydrolase enzymes: relevance to xenobiotic metabolism and toxicity. Crit Rev Toxicol 29(1):59–124

Wright MC, Maurel P, Paine AJ (1996) Induction of cytochrome P450 3A by metyrapone in human hepatocyte culture. Hum Exp Toxicol 15(3):203–204

Xie B, He X, Guo G et al (2020) High-throughput screening identified mitoxantrone to induce death of hepatocellular carcinoma cells with autophagy involvement. Biochem Biophys Res Commun 521(1):232–237